First-principles and spectroscopic studies of Bi(110) films: Thickness-dependent Dirac modes and property oscillations

G. Bian,[1,2,*] X. Wang,[3] T. Miller,[1,2] T.-C. Chiang,[1,2,†] P. J. Kowalczyk,[4,5] O. Mahapatra,[5] and S. A. Brown[5]

[1]*Department of Physics, University of Illinois at Urbana-Champaign, 1110 West Green Street, Urbana, Illinois 61801-3080, USA*

[2]*Frederick Seitz Materials Research Laboratory, University of Illinois at Urbana-Champaign, 104 South Goodwin Avenue, Urbana, Illinois 61801-2902, USA*

[3]*College of Science, Nanjing University of Science and Technology, Nanjing 210094, China*

[4]*Department of Solid State Physics, Faculty of Physics and Applied Informatics, University of Lodz, Pomorska 149/153, 90-236 Lodz, Poland*

[5]*The MacDiarmid Institute for Advanced Materials and Nanotechnology, Department of Physics and Astronomy, University of Canterbury, Private Bag 4800, Christchurch 8140, New Zealand*

(Received 9 June 2014; revised manuscript received 19 October 2014; published 7 November 2014)

The electronic structure of Bi(110) thin films as a function of film thickness is investigated by first-principles calculations, angle-resolved photoemission spectroscopy, and scanning tunneling microscopy. Energy minimization in the calculation reveals significant atomic relaxation and rebonding at the surface. The calculated surface energy for the relaxed structures indicates that films consisting of odd numbers of atomic layers are inherently unstable and tend to bifurcate into film domains consisting of neighboring even numbers of atomic layers. This theoretical trend agrees with experimental observations. The results can be explained by the presence of unsaturated p_z dangling bonds on the surfaces of films of odd-numbered atomic layers only. These p_z dangling bonds form a Dirac-cone feature near the Fermi level at the $\overline{M}$ point as a consequence of the interplay of mirror symmetry and spin-orbit coupling. Films consisting of even numbers of atomic layers exhibit a band gap at $\overline{M}$ instead.

DOI: 10.1103/PhysRevB.90.195409 PACS number(s): 71.70.Ej, 73.20.At, 73.21.Fg, 79.60.Dp

I. INTRODUCTION

Bismuth, with its large atomic spin-orbit coupling, is a key chemical element for constructing topological compound materials [1,2]. Bismuth by itself, in the form of thin films, has attracted considerable research interest due to the existence of competing structural phases and the interplay of strong spin-orbit interaction and quantum size effects [3–10]. Experimentally, epitaxial Bi ultrathin films have been grown on various substrates by molecular beam epitaxy. At film thicknesses less than about 2 nm, there are two distinctive allotropic structures. One is a hexagonal (HEX) phase, corresponding to the (111) orientation of the rhombohedral bulk phase of Bi. The other is a pseudocubic (PC) phase, corresponding to the (110) orientation of a somewhat distorted rhombohedral bulk phase. Interestingly, a Bi(111) single atomic layer (AL), also referred to as a Bi(111) bilayer in the literature because of its buckled graphene structure, possesses a nontrivial Z_2 topological order and hosts a quantum spin Hall state [11–13]. This system has been successfully prepared on Bi_2Te_3(111) substrates [14–17] and Sb thin films [18], where there is a nearly perfect lattice match. By contrast, (110)-oriented Bi films are topologically trivial [12], but this is the preferred or stable orientation when the film thickness is below a critical value that depends on the substrate material [6,19,20]. Prior studies have shown that epitaxial Bi(110) films exhibit a quasi-one-dimensional growth behavior and lateral quantum size effects [19]. The rich physics of Bi(110) films motivates the present paper.

This paper reports a study of the electronic structure and physical properties of Bi(110) thin films by first-principles calculations, scanning tunneling spectroscopy (STM), and angle-resolved photoemission spectroscopy (ARPES). The calculated surface energy shows that films made of even-numbered atomic layers (referred to as "even films" below for simplicity) are energetically favored relative to the odd films. Such even-odd differences or oscillations have been observed experimentally and reported previously [21]. However, the standard interpretation of such quantum oscillations in thin films in terms of the Fermi wave vector and one-dimensional shell filling does not apply [22]. Instead, the presence of unsaturated p_z dangling bonds on the surfaces of odd films of Bi(110) is the reason behind the phenomenon, as revealed by our first-principles calculations of the electronic structure. These p_z dangling bonds form a Dirac-cone feature at the $\overline{M}$ point of the surface Brillouin zone. This Dirac-cone feature is absent in even films and arises in odd films because of the strong spin-orbit coupling in Bi and the mirror symmetry of the (100) lattice.

II. METHODS

Our calculations of the electronic structure were performed using Hartwigsen-Goedecker-Hutter pseudopotentials [23] and a plane-wave basis set. The main program employed was developed by the ABINIT group [24,25]. Spin-orbit coupling was included, and densities of states were calculated by integrating over the entire Brillouin zone. The surfaces were relaxed for all film thicknesses, resulting in subtle but important differences in atomic arrangement compared to those reported in Ref. [3]. The optimized lattice parameters are given in Table I.

*Present address: Department of Physics, Princeton University, Jadwin Hall, Princeton, New Jersey, 08544, USA; gbian@princeton.edu

†tcchiang@illinois.edu

 ©2014 American Physical Society

TABLE I. Structural parameters of Bi(110) films with one- to eight-atomic-layer (AL, each AL consists of two sublayers) thickness: the interlayer distance $D_{i,j}$ of the sublayers i and j ($i = 1$ is the surface sublayer) derived from the ideal bulk structure is $D_{i,i+1} = 0.142$ and 3.087 Å for odd and even i, respectively. The in-plane displacements of the atoms after the lattice optimization with respect to the bulk structure were found to be negligible. Substantial lattice relaxation is found to happen only within the top three sublayers.

Distance (Å)	1 AL	2 AL	3 AL	4 AL	5 AL	6 AL	7 AL	8 AL
D_{12}	0.600	−0.001	−0.313	−0.149	−0.054	−0.074	−0.033	−0.022
D_{23}		3.017	3.188	3.045	3.046	3.026	3.026	3.023

A vacuum layer of 20 Å thickness is employed in the density functional theory (DFT) slab calculation. The cutoff energy is 350 eV.

Samples were prepared by evaporation of Bi onto cleaved, highly oriented pyrolytic graphite (HOPG), which was subsequently transferred for ARPES, STM, or noncontact (NC)-atomic force microscopy (AFM) measurements under ultrahigh-vacuum throughout the process. The base pressure of the ARPES measurement is better than 10^{-10} Torr. The energy resolution in the ARPES measurements is equal to or better than 15 meV. The deposition rate was measured by a quartz thickness monitor. Photoemission measurements of the band structure were performed at the Synchrotron Radiation Center of the University of Wisconsin at Madison using 22 eV photons and a hemispherical analyzer (Scienta SES-100) equipped with a two-dimensional detector. Details about STM imaging are given in Refs. [26] and [27]. Typical bias voltage and tunneling current were −0.8 V and 50 pA, respectively.

III. RESULTS AND DISCUSSION

The rhombohedral bulk structure of Bi can be described as a face-centered-cubic structure stretched along the body diagonal [6]. The HEX phase, corresponding to Bi(111), is the preferred structure for thicker films. The PC phase, corresponding to Bi(110), tends to be more stable at smaller film thicknesses; it is also referred to as a black-phosphorus-like structure in the literature [6,21,28]. The experimentally observed critical thickness for PC-HEX crossover is about 6 AL for films grown on Si(111) and 12 AL for HOPG. The PC phase has a lower surface energy, which makes it the preferred structure at small thicknesses. This surface effect diminishes with increasing film thickness, and thicker films tend to adopt the HEX phase for its lower bulk energy [6,20]. The atomic structure of Bi(110) is shown in Figs. 1(a) and 1(b). The surface has a quasisquare unit cell, and each AL consists of two sublayers with a small vertical buckling of 0.14 Å. The surface Brillouin zone is presented in Fig. 1(c). Figure 1(d) shows an STM image of a Bi(110) film grown on HOPG; it agrees with the structure shown in Fig. 1(a).

The calculated band structures of freestanding Bi(110) films with theoretically optimized surface structure for thicknesses ranging from 1 to 8 AL are presented in Fig. 2. The shaded regions represent projected bulk bands highlighting the bulk band gap around the Fermi level. The states within the bulk band gap can be regarded as "surface states" of the thin films. The number of bands (quantum well subbands) increases for increasing film thickness. In the bulk limit, most of the subbands should merge into the bulk band continuum, but isolated subbands can remain in the bulk gap and form surface states. For odd films, there exists a Dirac-cone feature near the Fermi level at the surface Brillouin zone corner $\overline{M}$, as marked by a dashed rectangle in each case in Fig. 2; this feature is conspicuously missing for the even films. It originates from the dangling p_z orbitals on the surface. Each Bi atom has five valence electrons, and its coordination number must be 3 in order to reach a full shell. This is the case for bulk Bi, but not necessarily at the surface. The calculated total charge densities of Bi(110) films (Fig. 3) reveal that the coordination number for the surface atoms in the odd films is only 2. The unbonded electron gives rise to a dangling p_z orbital, as indicated by a dashed line, where a solid line indicates a regular interatomic bond. The corresponding band is half filled and forms a Dirac cone at the Fermi level in much the same way as the π band of graphene. In the even films, there is significant bonding between the surface atomic layer and the atomic layer below through lattice relaxation. This interlayer bonding stabilizes the structure and removes the dangling bond and the Dirac-cone feature.

To further clarify the different bonding configurations between even and odd films, we show in Fig. 4 the charge density distributions of states A–F associated with 1 and 2 AL films as marked in Fig. 2. States A and B for the 1 AL film show charge densities indicative of a dangling p_z orbital; this agrees with the assignment of the Dirac cone to the dangling bond. By contrast, the p_z orbitals for the 2 AL film of interest can pair up with the same orbitals in the other atomic layer, thus restoring the atomic coordination number to 3.

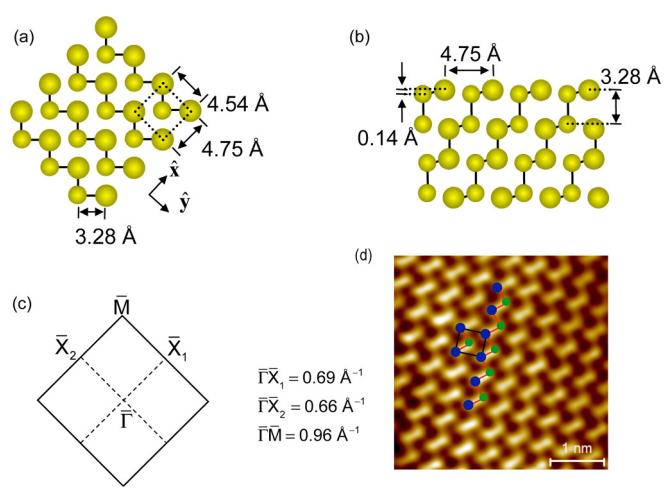

FIG. 1. (Color online) Schematic lattice structure of Bi(110): (a) top view and (b) side view along the −ŷ direction. (c) Surface Brillouin zone. (d) High-resolution STM image. A PC unit cell is indicated.

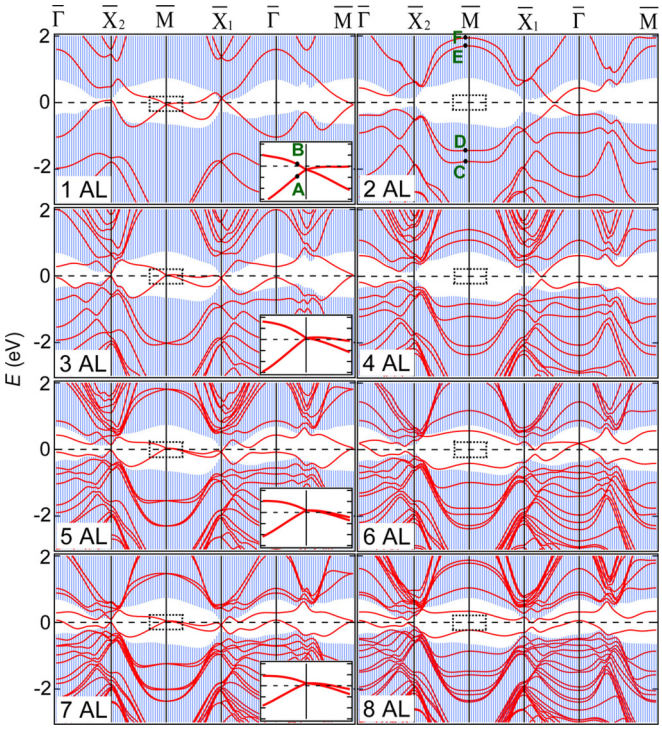

FIG. 2. (Color online) Band structure of Bi films of thickness 1 to 8 AL. The insets for the odd films show enlarged views of the area enclosed by the dashed rectangles. The shaded regions represent projected bulk bands highlighting the bulk band gap around the Fermi level.

Specifically, the occupied bonding states C and D correspond to large charge accumulation between the two atomic layers, as seen in Fig. 3, which indicates interlayer covalent bonding. It is important to note that this bonding is made possible by

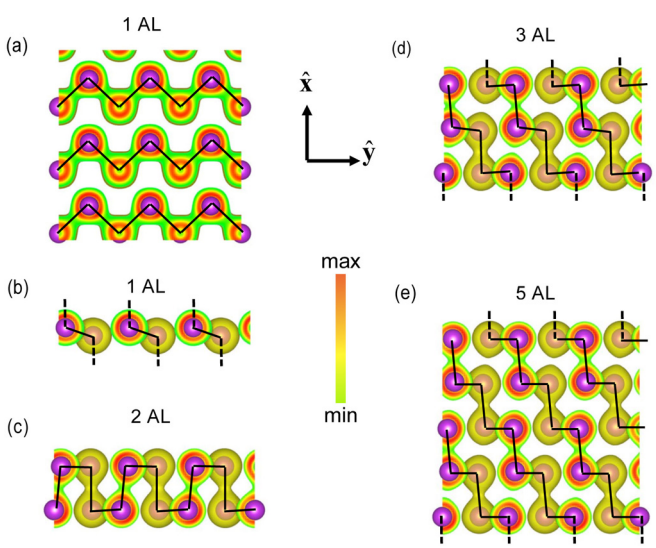

FIG. 3. (Color online) Calculated total charge densities of Bi(110) films. (a) Top view and (b) side view along ŷ of 1 AL Bi(110) film. (c)–(e) Side views of films of thickness 2, 3, and 5 AL. Interatomic bonds and dangling bonds are indicated by solid and dashed lines, respectively.

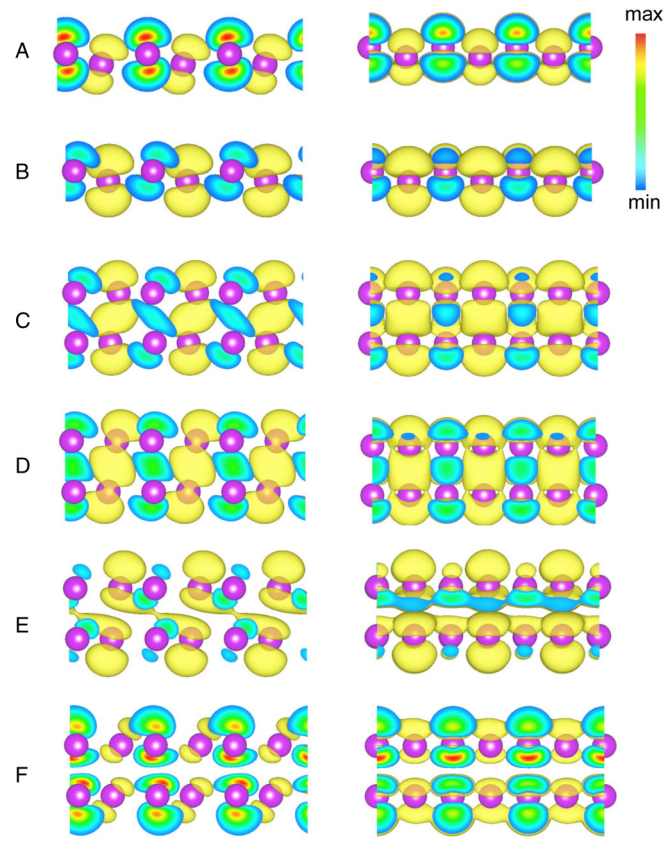

FIG. 4. (Color online) Charge densities of states A–F (indicated in Fig. 2) near $\overline{M}$. The left and right panels are side views along the ŷ and x̂ directions, respectively.

significant relaxation of the atomic positions in the calculation by total energy minimization. Physically, dangling bonds are high-energy objects, and the system adjusts its atomic positions to avoid them as much as possible. The antibonding states E and F are derived from destructive superposition of the p_z orbitals in between the atomic layers, and they are left unoccupied above the Fermi level.

This interlayer bonding mechanism for dangling bond removal and energy minimization cannot happen for a 3 AL film. To do so, both the top and bottom atomic layers would need to form covalent bonds with the middle atomic layer, but that would lead to overbonding of the middle atomic layer, which is energetically unfavorable. The same argument applies to thicker odd films. As the film thickness becomes large enough, this surface effect diminishes. In fact, the system tends to adopt the bulk (111) configuration above the critical thickness because of its lower bulk energy.

Figure 5 presents the surface energy and bifurcation energy of Bi(110) films of 1–8 AL. The surface energy is defined as the total film energy subtracted by the corresponding bulk energy, which is determined from the slope of the slab energy as a function of film thickness. The bifurcation energy of an n AL film is defined as $B_n = 2E_n - E_{n+1} - E_{n-1}$, where E_n is the total energy of the n AL film. If this energy is negative, the n AL film would tend to bifurcate into a combination of $(n + 1)$ and $(n - 1)$ AL film domains in order to reduce the total energy of the system. This differential quantity is a

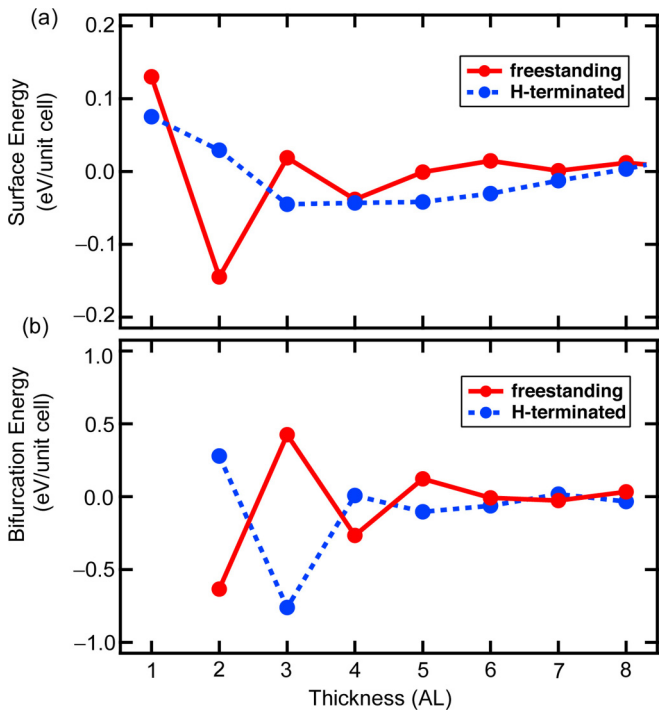

FIG. 5. (Color online) (a) Surface energy of Bi(100) films as a function of thickness: solid lines for freestanding films and dashed lines for H-terminated films. (b) Bifurcation energy of Bi(100) films as a function of thickness.

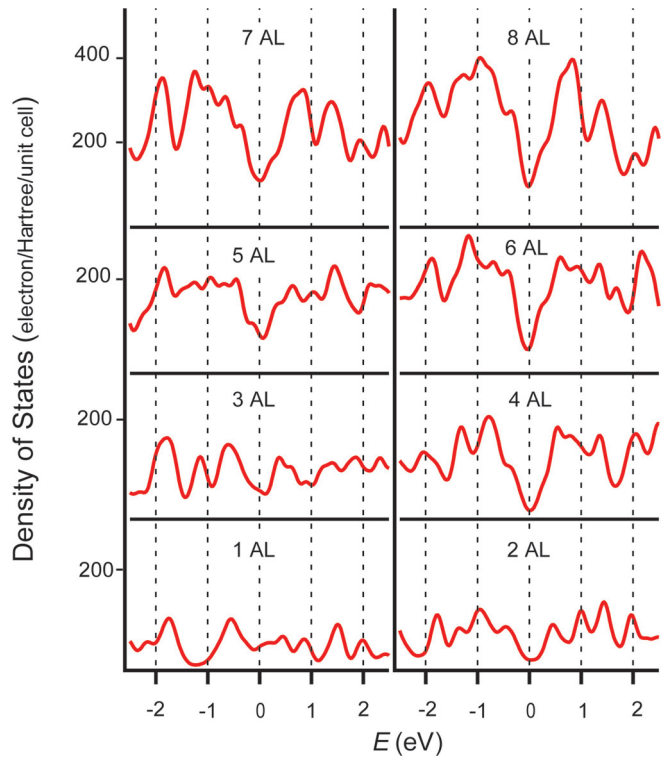

FIG. 6. (Color online) DOS of Bi(110) films for different thicknesses.

more sensitive measure of the energies of the system. Both the surface energy and bifurcation energy show an even-odd oscillatory behavior at thicknesses below 6 AL. The even films are energetically favored compared to the adjacent odd films because of the energy reduction involving interlayer rebonding and dangling bond removal.

For comparison, we have also calculated the surface and bifurcation energies for films with one surface terminated by hydrogen atoms. One H atom is initially placed right above each Bi atom on the top surface of the film, and the atomic positions are optimized subsequently. The results are shown in Fig. 5 by the dotted lines. The even-odd oscillatory trend in the bifurcation energy is now flipped compared to the pristine films. The reason is that the H atoms saturate the dangling bonds on the terminated surface, which reduces the surface energy of odd films while hindering pair-up of neighboring atomic layers in the even films.

Shown in Fig. 6 are the density of states (DOS) of Bi(110) slabs of various thicknesses. The DOS was calculated by counting the number of states over the entire Brillouin zone. The odd films possess higher DOS around the Fermi level compared to the even films. The trend reflects the existence of the partially occupied dangling bond bands on the surfaces of odd films.

Images taken by scanning electron microscope (SEM) and NC-AFM of Bi(110) films grown on HOPG at room temperature are shown in Figs. 7(a) and 7(b), respectively. When the coverage is low, the deposited Bi atoms arrange into flakes/islands in multiple domains. The preferred thicknesses are "2 + 1," "4 + 1," and "6 + 1" AL, where "1" represents the 1 AL thick wetting or "dead" AL, which serves as an inert buffer on HOPG to support the growth of Bi(110) films [19]. The islands are elongated along the Bi[1$\bar{1}$0] direction [which corresponds to the y direction in Fig. 1(a)], with preferred periodic widths as a result of lateral quantum size effects [19]. With increasing deposition of Bi, the islands connect and merge into a nonuniform film. The preferred thicknesses are consistent with our calculated bifurcation energies if the wetting AL is excluded. This result can be explained by the different chemical bonding environment of the bottom Bi AL; its bonding to the substrate has an effect similar to H-termination as discussed above.

For ARPES measurements, we tried to make the films as smooth and uniform as possible by depositing Bi onto HOPG at 60 K and then annealing the film to 350 K. This yields smoother but not perfectly smooth films based on extensive experimentation. The ARPES spectra for different amounts of Bi deposition are shown in Fig. 7(c), together with the calculated band structure and the second derivative of the raw data to enhance the visibility of the bands. It is evident that these films do not have uniform thicknesses. Bands for different energetically favored thicknesses coexist in the ARPES spectra. The Fermi level is shifted relative to the computed results, possibly due to a charge transfer between the film and the substrate. Nevertheless, the photoemission data are generally consistent with the calculation.

The formation of the Dirac-cone feature at $\overline{M}$ for odd films is closely related to the strong atomic spin-orbit coupling of Bi and the mirror symmetry of the lattice. Without loss of generality, we will discuss only the 1 AL case. The lattice structure is shown in Figs. 3(a) and 3(b). This structure is

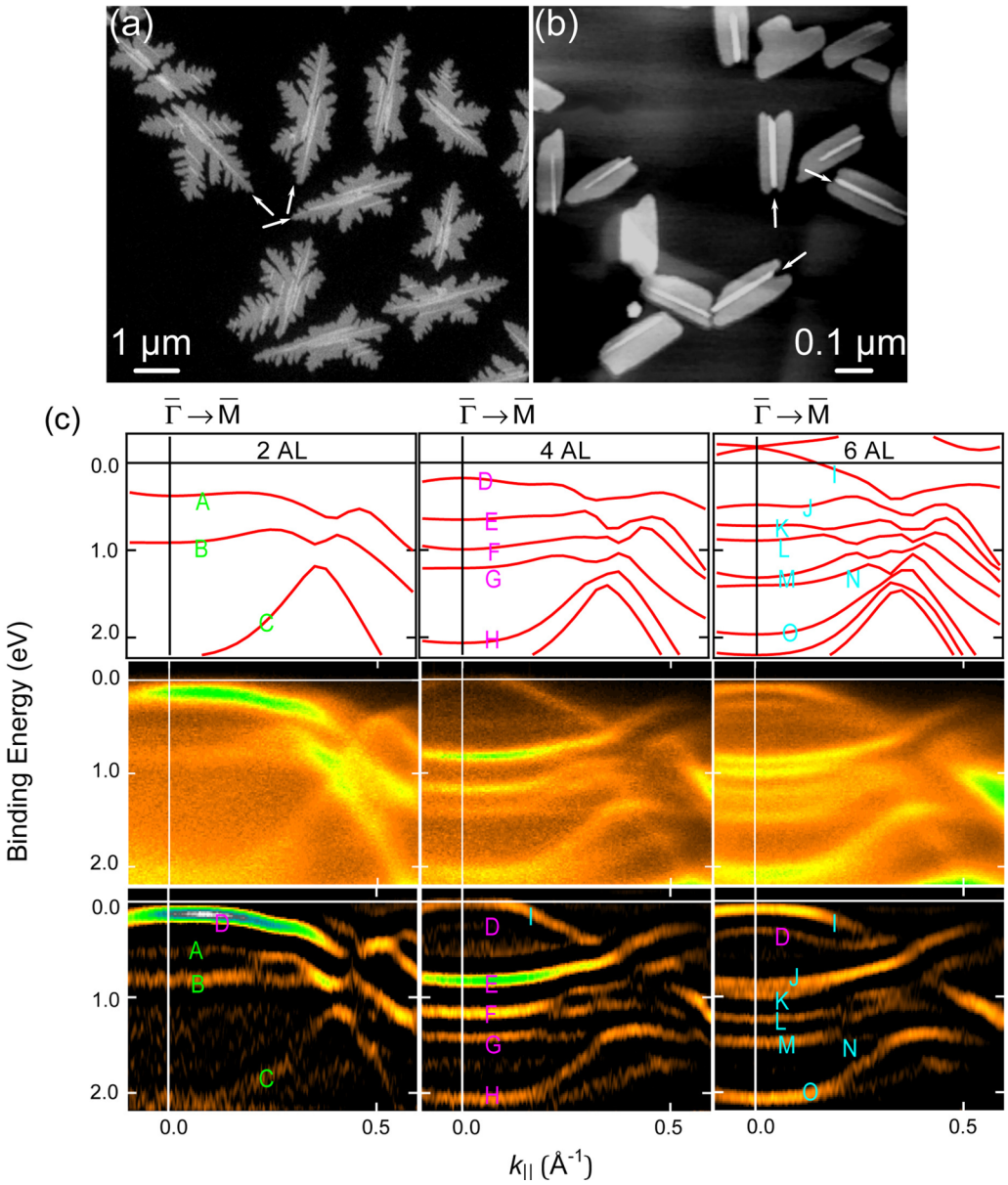

FIG. 7. (Color online) (a) SEM and (b) NC-AFM images of Bi(110) films grown on HOPG. (c) Top panels: Band structure of Bi(110) films of thickness 2, 4, and 6 AL. Middle panels: ARPES data. Bottom panels: Second derivative of the ARPES data.

invariant under spatial inversion about the midpoint between the two Bi atoms in a unit cell. Given the system is invariant under time reversal as well, each electronic state is doubly degenerate with respect to the electron spin. This structure is also symmetric with respect to a mirror plane perpendicular to $\hat{y}$; here, $\hat{x}$ and $\hat{y}$ are unit vectors along $\overline{\Gamma}\,\overline{X_1}$ and $\overline{\Gamma}\,\overline{X_2}$, respectively (see Fig. 1). The band structure for the 1 AL film in its optimized structure is presented in Fig. 8(a). The inset shows a schematic drawing of the atomic structure; its mirror symmetry with respect to the xz plane is evident. The mirror plane maps $\overline{X_1}$ and $\overline{M}$ to equivalent k points, but not $\overline{X_2}$. The two bands derived from the dangling p_z orbitals cross each other at $\overline{X_1}$ and $\overline{M}$, but they do not cross at $\overline{X_2}$ because of the lack of mirror symmetry with respect to the yz plane. Such band crossings are a robust feature independent of the x-position of the atom within the unit cell, as shown in Fig. 8(a). We note that there is no hybridization gap at the crossing point from the coupling between the two surfaces of thin slabs. This is due to the fact that the two branches at the band crossing have opposite mirror parity eigenvalues; therefore, the gap opening is not allowed at mirror-invariant k points such as $\overline{X_1}$ and $\overline{M}$. The physics is similar to the crystalline symmetry protection mechanism of the band crossings discussed under the framework of topological crystalline insulators [29] and three-dimensional Dirac semimetals [30–33]. However, if the mirror symmetry is broken, as illustrated in Fig. 8(c), an energy gap shows up at the band crossing points. On the other hand, if we enforce a mirror symmetry with respect to the yz plane, the gap at $\overline{X_2}$ closes, as shown in Fig. 8(d). Thus, the mirror symmetry "protects" the Dirac-cone feature from gap opening. For reference, we also consider the case where the spin-orbit coupling is turned off in the calculation, and the results are shown in Fig. 8(b) for the undistorted structure. The two bands along $\overline{M}\,\overline{X_1}$ now collapse into a single band. Evidently, the

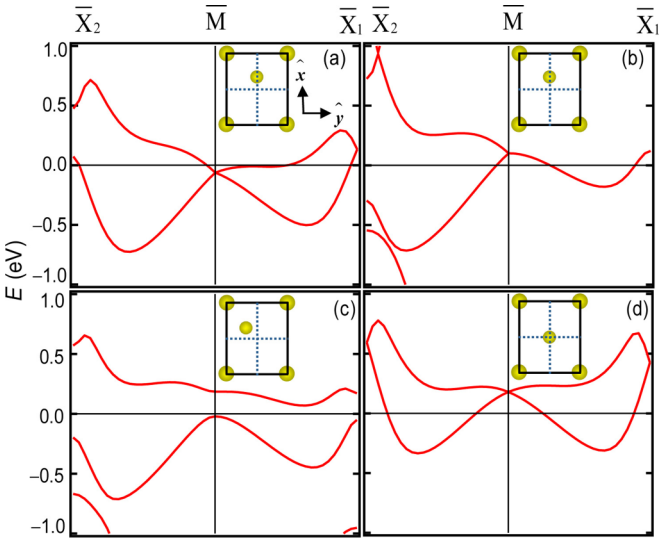

FIG. 8. (Color online) Band structure of a 1 AL Bi(110) film (a) with and (b) without spin-orbit coupling. (c) Band structure of a distorted 1 AL lattice without any mirror symmetry. (d) Band structure of a lattice with two mirror planes. Insets show schematically the lattice in each case.

strong atomic spin-orbit coupling is essential for maintaining the Dirac-cone feature around the zone corner $\overline{M}$. This is different from the π band of graphene, for which the effects of spin-orbit coupling are negligible. These results suggest a platform for investigating Dirac modes in two-dimensional systems under strong spin-orbit coupling.

IV. CONCLUSIONS

In summary, we have examined the electronic structure and properties of Bi(110) films by first-principles calculations, ARPES, and STM. Experimental Bi(110) thin films were prepared on the cleaved surface of HOPG. The calculated surface energy shows an oscillatory behavior with a period of 2 AL, which is in good accord with STM and APRES observations of the system's preference for even films. This phenomenon can be explained by the presence of dangling p_z orbitals on the surfaces of odd films, whereas in even films, the dangling bonds are removed through interlayer bonding. Even though the odd films are not energetically favorable, they host low-energy Dirac modes at the surface Brillouin zone corner that arise from the dangling orbitals on the surface. The Dirac modes are a consequence of a mirror symmetry of the lattice. Unlike the case of graphene, the intrinsic strong spin-orbit coupling of Bi atoms plays a key role in the formation of the two-dimensional Dirac cone. Our results provide a promising indication of device applications of Bi(110) thin films.

ACKNOWLEDGMENTS

T.-C.C. acknowledges support from the U.S. Department of Energy (Grant No. DE-FG02–07ER46383). P.J.K., O.M., and S.A.B. acknowledge support from The MacDiarmid Institute for Advanced Materials and Nanotechnology. X.W. acknowledges financial support by the Natural Science Foundation of China (Grant No. 11204133) and the Jiangsu Province Natural Science Foundation of China (Grant No. BK2012393). The Synchrotron Radiation Center was supported by the National Science Foundation.

[1] M. Z. Hasan and C. L. Kane, Rev. Mod. Phys. **82**, 3045 (2010).
[2] X.-L. Qi and S.-C. Zhang, Rev. Mod. Phys. **83**, 1057 (2011).
[3] Yu. M. Koroteev, G. Bihlmayer, E. V. Chulkov, and S. Blügel, Phys. Rev. B **77**, 045428 (2008).
[4] P. Hofmann, Prog. Surf. Sci. **81**, 191 (2006).
[5] S. Agergaard, C. Søndergaard, H. Li, M. B. Nielsen, S. V. Hoffmann, Z. Li, and P. Hofmann, New J. Phys. **3**, 15 (2001).
[6] G. Bian, T. Miller, and T.-C. Chiang, Phys. Rev. B **80**, 245407 (2009).
[7] S. Yaginuma, T. Nagao, J. T. Sadowski, M. Saito, K. Nagaoka, Y. Fujikawa, T. Sakurai, and T. Nakayama, Surf. Sci. **601**, 3593 (2007).
[8] T. Hirahara, T. Nagao, I. Matsuda, G. Bihlmayer, E. V. Chulkov, Yu. M. Koroteev, P. M. Echenique, M. Saito, and S. Hasegawa, Phys. Rev. Lett. **97**, 146803 (2006).
[9] S. Hatta, Y. Ohtsubo, S. Miyamoto, H. Okuyama, and T. Aruga, Appl. Surf. Sci. **256**, 1252 (2009).
[10] C. R. Ast and H. Höchst, Phys. Rev. B **67**, 113102 (2003).
[11] S. Murakami, Phys. Rev. Lett. **97**, 236805 (2006).
[12] M. Wada, S. Murakami, F. Freimuth, and G. Bihlmayer, Phys. Rev. B **83**, 121310(R) (2011).
[13] Z. Liu, C.-X. Liu, Y.-S. Wu, W.-H. Duan, F. Liu, and J. Wu, Phys. Rev. Lett. **107**, 136805 (2011).
[14] T. Hirahara, G. Bihlmayer, Y. Sakamoto, M. Yamada, H. Miyazaki, S.-i. Kimura, S. Blügel, and S. Hasegawa, Phys. Rev. Lett. **107**, 166801 (2011).
[15] M. Chen, J.-P. Peng, H.-M Zhang, L.-L. Wang, K. He, X.-C. Ma, and Q.-K. Xue, Appl. Phys. Lett. **101**, 081603 (2012).
[16] F. Yang, L. Miao, Z. F. Wang, M.-Y. Yao, F. Zhu, Y. R. Song, M.-X. Wang, J.-P. Xu, A. V. Fedorov, Z. Sun, G. B. Zhang, C. Liu, F. Liu, D. Qian, C. L. Gao, and J.-F. Jia, Phys. Rev. Lett. **109**, 016801 (2012).
[17] N. Fukui, T. Hirahara, T. Shirasawa, T. Takahashi, K. Kobayashi, and S. Hasegawa, Phys. Rev. B **85**, 115426 (2012).
[18] G. Bian, T. Miller, and T.-C. Chiang (unpublished).
[19] P. J. Kowalczyk, O. Mahapatra, S. A. Brown, G. Bian, X. Wang, and T.-C. Chiang, Nano Lett. **13**, 43 (2013).
[20] S. A. Scott, M. V. Kral, and S. A. Brown, Surf. Sci. **587**, 175 (2005).
[21] T. Nagao, J. T. Sadowski, M. Saito, S. Yaginuma, Y. Fujikawa, T. Kogure, T. Ohno, Y. Hasegawa, S. Hasegawa, and T. Sakurai, Phys. Rev. Lett. **93**, 105501 (2004).
[22] T. Miller, M. Y. Chou, and T.-C. Chiang, Phys. Rev. Lett. **102**, 236803 (2009).
[23] C. Hartwigsen, S. Goedecker, and J. Hutter, Phys. Rev. B **58**, 3641 (1998).

[24] X. Gonze, J.-M. Beuken, R. Caracas, F. Detraux, M. Fuchs, G.-M. Rignanese, L. Sindic, M. Verstraete, G. Zerah, F. Jollet, M. Torrent, A. Roy, M. Mikami, P. Ghosez, J.-Y. Raty, and D. C. Allan, Comput. Mater. Sci. **25**, 478 (2002).
[25] X. Gonze, G.-M. Rignanese, M. Verstraete, J.-M. Beuken, Y. Pouillon, R. Caracas, F. Jollet, M. Torrent, G. Zerah, M. Mikami, Ph. Ghosez, M. Veithen, J.-Y. Raty, V. Olevano, F. Bruneval, L. Reining, R. Godby, G. Onida, D. R. Hamann, and D. C. Allan, Zeit. Kristallogr. **220**, 558 (2005).
[26] D. N. McCarthy, D. Robertson, P. J. Kowalczyk, and S. A. Brown, Surf. Sci. **604**, 1273 (2010).
[27] P. J. Kowalczyk, O. Mahapatra, D. McCarthy, W. Kozlowski, Z. Klusek, and S. A. Brown, Surf. Sci. **605**, 659 (2011).
[28] S. Yaginuma, K. Nagaoka, T. Nagao, G. Bihlmayer, Yu. M. Koroteev, E. V. Chulkov, and T. Nakayama, J. Phys. Soc. Jpn. **77**, 014701 (2008).
[29] L. Fu, Phys. Rev. Lett. **106**, 106802 (2011).
[30] B.-J. Yang and N. Nagaosa, Nat. Commun. **5**, 4898 (2014).
[31] X. Wan, A. M. Turner, A. Vishwanath, and S. Y. Savrasov, Phys. Rev. B **83**, 205101 (2011).
[32] Z. Wang, Y. Sun, X.-Q. Chen, C. Franchini, G. Xu, H. Weng, X. Dai, and Z. Fang, Phys. Rev. B **85**, 195320 (2012).
[33] S. M. Young, S. Zaheer, J. C. Y. Teo, C. L. Kane, E. J. Mele, and A. M. Rappe, Phys. Rev. Lett. **108**, 140405 (2012).